

**SHAPE PERCEPTION OF CLEAR WATER IN  
PHOTO-REALISTIC IMAGES**

ARHUM SULTANA

A THESIS SUBMITTED TO THE FACULTY OF GRADUATE STUDIES  
IN PARTIAL FULFILMENT OF THE REQUIREMENTS  
FOR THE DEGREE OF  
MASTER OF APPLIED SCIENCE

GRADUATE PROGRAM IN ELECTRICAL ENGINEERING AND COMPUTER SCIENCE  
YORK UNIVERSITY  
TORONTO, ONTARIO

March 2017

©Arhum Sultana, 2017

## **ABSTRACT**

Light plays a vital role in the perception of transparency, depth and shape of liquids. The perception of the surfaces of liquids is made possible with an understanding of refraction of light and knowledge of the underlying texture geometry. Given this, what specific characteristics of the natural optical environment are essential to the perception of transparent liquids, specifically with respect to efficiency and realism? In this thesis, a light path triangulation method for the recovery of transparent surface shape and a system to estimate the perceived shape of any arbitrary-shaped object with a refractive surface are proposed. A psychophysical experiment was conducted to investigate this using the perceived shape of water from stereo images using a real time stereoscopic 3-D depth gauge. The results suggest that people are able to consistently perceive shape of liquids from photo-realistic images and that regularity in underlying texture facilitates human judgements of surface shape.

To my mother for her persistent love...  
And to my sisters for their continual support...

Thank you

## **Acknowledgement**

My first deepest Thank is for my supervisor Prof. Robert Allison. It has been an honor to work with him as my true research guide both on scientific and personal level while living here in Canada. He made me learn great ways to present ideas, understand questions and solve problems. He was so consistent in sorting away my confusions and queries during all my research time and writing of this thesis. I appreciate his support to contribute his time, ideas and patience to make my master's experience stimulating and useful one. I could not have imagined having a better advisor and mentor for my MaSc study.

I would like to appreciate my committee members, York's body and all the faculty and non-faculty members for their support. Without their presence, insight, encouragement and hard questions, this work would hardly have been completed.

I would also like to reflect on our Percept lab group, friends and colleagues for their stimulating discussions and sharing of two year's pleasant research life.

And of course my mother (being far) who always help me during the moments of fears, who is always ready to enlighten me in searching ways and showing right attitude to stay determined in reaching my goals.

May God bless each one of you!

## TABLE OF CONTENTS

<b>Abstract.....</b>	<b>ii</b>
<b>Dedication.....</b>	<b>iii</b>
<b>Acknowledgement.....</b>	<b>iv</b>
<b>Table of Contents.....</b>	<b>v</b>
<b>List of Figures.....</b>	<b>viii</b>
<b>List of Equations.....</b>	<b>xi</b>
<b>1 Introduction</b>	<b>1</b>
1.1 Motivation.....	1
1.2 Contributions.....	2
1.3 Thesis outline.....	3
<b>2 Literature Review</b>	<b>5</b>
2.1 Local Surface Geometry and Optical Information.....	6
2.2 Stereoscopic and Non-Stereoscopic view.....	14
2.3 Rendering approximations.....	15
2.4 Non-Linearity and bas-relief using Gauge Figure task.....	16
2.5 Summary.....	17
<b>3 Water Optics and 3-D Simulation</b>	<b>18</b>
3.1 Physical and Optical Properties of Water.....	18
3.2 Water Simulation in 3-D.....	21
3.3 Imaging of water surfaces.....	21

3.4	Light-Path Triangulation.....	24
<b>4</b>	<b>Experiment and Analysis</b>	<b>27</b>
4.1	Methods.....	27
4.1.1	Apparatus.....	28
4.1.2	System Software.....	30
4.2	Subjects and experimental sessions.....	31
4.2.1	Stimuli and Conditions.....	31
4.2.2	Experiment Procedure .....	35
4.3	Results and Discussion.....	37
4.3.1	How well do humans perceive the shape of transparent objects?.....	37
4.3.2	Do cues from textures provide useful information to perceive..... shape?.....	41
4.3.3	Which areas had larger perceptual errors and why?.....	43
4.4	Discussion.....	46
4.5	Limitations.....	47
4.5.1	Differences of perception from stereoscopic images & real world..... objects .....	47
4.5.2	Different transparent objects with range of texture maps.....	48
4.5.3	Gauge probe task control.....	48

<b>5</b>	<b>Conclusion and Future Work</b>	<b>50</b>
5.1	Future Work.....	51
	<b>Bibliography</b>	<b>52</b>

## LIST OF FIGURES

2.1	Color-coded angular errors. For surface shape estimation, the analysis defines perceived shape of a Lambertian surface with homogenous illumination. The red dots represent the highest marked errors and blue being lowest. [Todd <i>et al.</i> , 2014].....	07
2.2(a)	The stimuli of specular mirror surfaces [Fleming <i>et al.</i> , 2004] showing stationary images with reflected environment and their respective edge-detection maps .....	08
2.2(b)	Plots pooled across two shapes, illuminations and subjects. The green line shows ideal performances, red line represents the best-fit of linear regression whereas light blue dots indicate the tilt estimates for which slant is less than $15^\circ$ (i.e., objective tilt is ill-defined) .....	08
2.3	Experiment images used by [Kim <i>et al.</i> , 2016].Refractive rating shows the strength of opacity and degree of transparency. ....	10
2.4	Represents Depth and Normal maps for three different time sequences of water-flow estimations to characterize shape distortion (pour and ripple formations respectively). [Morris <i>et al.</i> , 2013] .....	13

3.1	Change in the direction of a light due to change in water density. [Adapted from Gettys W. Edward <i>et al.</i> , 1989].....	20
3.2	Geometry of underwater refraction: Face-on-view to determine the hypothetical depth ( $z$ distance) from the vertex of $p$ . [Adapted from Morris 2004].....	23
3.3	Imaging Model: $D1$ and $D2$ are both refracted at point $P$ and imaged in the two cameras at point $C1$ and $C2$ respectively. The rays triangulate in identical manner to intersect water surface and ensure common surface normal $n$ for each unique surface point $P$ . The approach can be used for Binocular Stereo Vision to reconstruct 3-D surface points in order to estimate object's shape[Adapted from Morris 2004] .....	26
4.1	A set of circular figures arranged on a sphere to illustrate the slant [ $0 < \Theta < 2\pi$ ] and tilt [ $0 < \theta < \pi$ ] components of surface orientation based on circular gauge probe .Note that the line at the center of each patch is aligned with the direction of the surface normal [Normal <i>et al.</i> , 2005] .....	28
4.2	Experimental set up with a subject performing task to judge surface shape disparity using mouse by adjusting overlaid S3D glyph indicating surface-normal. The viewing distance was about 69.8cm.....	29

4.3(a)	Stimuli objects of changing water surface placed over regular and noisy base textures.....	33
4.3(b)	Depth maps & Normal maps for corresponding stimuli in tangential space.....	34
4.4	Screen shot of gauge figure. Subject adjusting the overlaid probe at the surface of one of the stimuli.....	36
4.5	Average estimation errors and confidence intervals (95%) for each subject and viewing condition. ....	38
4.6	Average estimation errors and confidence intervals (95%) for each shape by each subject.....	40
4.7	Average estimation errors & confidence intervals (95%) for each texture by each subject.....	42
4.8a	Largest and high frequency sorted errors of ripple shape under regular texture pattern.....	44
4.8b	Largest and high frequency sorted errors of wave shape under regular texture pattern.....	45

## LIST OF EQUATIONS

3.1	$\mu_1 \sin (\Theta_1) = \mu_2 \sin (\Theta_3)$ .....	19
3.2	$\sin (\Theta_1) = 1.33 \sin (\Theta_3)$ .....	20
3.3	$\frac{\ p-c\ }{\sin(\theta_2-\beta)} = \frac{\ d-c\ }{\sin(\theta_1-\theta_2+\pi)}$ .....	22
5.1	Angular error = $\cos^{-1}(\text{nes} \cdot \text{ngt})$ .....	37

# **Chapter 1 Introduction**

## **1.1 Motivation**

Water in its all three states has been a source of inspiration to all fields of arts, science, poetry and philosophy. The transparent nature of water, its visual dynamics which it reveals as a free flowing liquid and the unique physical chemistry behind this deceptively simple diatomic molecular substance motivated and inspired me to dive into exploring the underlying science of its shape.

In our modern digital world, individuals often view renderings of beautiful transparent 3-D objects in games, art and cinema. Consequently, computer-generated water and other fluids have received considerable practical and research attention. For me the questions of interest are: How are humans able to visualize and make sense of the shape and texture of water in the real world? What specific information needs to be provided to the user to render the transparency of water in 3-D efficiently while supporting effective visual shape perception? Visual shape perception is a formidably complex task for transparent objects.

I also considered the role of stereoscopic vision in this process. Stereoscopic vision is the process of recovering shape and depth in three-dimensional environments based on the differences or disparities between the left and right eye's images. Stereoscopy can create vibrant, visually plausible realistic 3-D scenes on computer displays.

This thesis studies the visual cues involved in shape perception of water in 3-D virtual worlds using psychophysical measurements. I consider whether stereopsis can contribute to the tasks of (1) identifying the shape of still surfaces which are transparent in nature (2) effectively rendering 3-D transparent surfaces and (3) providing quantitative estimates of the orientation of surface patches. I hypothesize that displays that support binocular stereovision will produce reduced shape estimation errors compared to equivalent monocular non-stereoscopic displays for similar shapes.

## **1.2 Contribution**

I present an experimental system based on Chen and Allison [2013], which combines pre-rendered photo-realistic stereoscopic images and a real-time gauge adjustment task to estimate the perceived orientation of surface shape at arbitrary locations in the image.

This thesis contributes to the areas of human visual perception and perceptually guided rendering by:

- 1) Developing a system that renders the photo-realistic shape of a volume of water in static 3-D virtual scenes characterized by the physics of light path transport phenomenon.
- 2) Testing the hypothesis that rendering of objects in a 3-D scene with stereopsis increases fidelity and improves the accuracy of shape judgments. This has practical importance for precise simulation of transparent objects.

- 3) Exploring the effects of texture backgrounds and how they contribute to the estimates of the surface geometries associated with foreground water shapes.
- 4) Explaining the orientation estimation errors in terms of the information contained in the image.

On the basis of the mathematical analysis and physical laws, I predict that humans have the necessary information to perceive the possible shapes of water surfaces with underlying textures; given certain constraints. The experiments aim to evaluate whether humans can identify and reconstruct the shape of transparent objects in refractive stereo given that:

- i. The scene redirects incoming light just once and the index of refraction is known.
- ii. Surface of water is optically smooth and transparent
- iii. At least two viewpoints should be available to obtain one 3-D point on its light path at viewing surface.

### **1.3 Thesis Outline**

The thesis consists of 5 chapters. Following this Introduction, I review related work in the fields mentioned above to describe the processes of image formation and image understanding underlying human shape judgments in the presence of transparency. I emphasize the importance of local surface information in order to reconstruct the transparent shape of an object in stereoscopic display. The third chapter presents the

mathematics underlying the computational vision problem of transparent shape estimation. I discuss how I approached the problem, based on scene composition in a 3-D work-frame, and how the feasibility of stereoscopic shape reconstruction is affected by variables such as reflective highlights on the surface, the lighting conditions, viewing conditions and other factors. These analyses lead to theoretical predictions about the feasibility and reliability of stereoscopic transparent shape perception.

The fourth chapter tests these theoretical predictions experimentally with human observers. Shape perception of transparent objects in stereoscopic versus non-stereoscopic conditions was compared for carefully chosen test conditions. The chapter also discusses the findings and their implication for models of human stereoscopic shape perception and for effective 3-D surface rendering.

The final chapter summarizes the conclusions and possible future work related to this study.

## Chapter 2 Literature Review

Shape estimation of transparent objects is a well-known phenomenon, however, little is known about how humans estimate the surface shapes of water and other liquids. Although shape reconstruction of transparent objects is an ambiguous problem, the human visual system is known to produce a coherent percept of shape change [Langer *et al.*, 2000] and is able to reconstruct a 3-D shape from refracted pre-rendered images [Chen *et al.*, 2013, Pasqualotto *et al.*, 2008].

In this review, I will focus on four major issues which emerge repeatedly throughout the literature I reviewed in order to understand the problem of shape reconstruction particularly for transparent liquids from static images. These issues are:

(1) Effects of local surface geometry [Enright *et al.*, 2002, Peachy *et al.*, 1986, Foster *et al.*, 1995, Todd *et al.*, 2014, Fleming *et al.*, 2004, Kim *et al.*, 2016; Ueda *et al.*, 2015; Schluter *et al.*, 2014] (2) Comparative study between viewing conditions [Morris *et al.*, 2011; Enright *et al.*, 2002; Shemdin 1990; Kersten *et al.*, 2006; Bridge *et al.*, 2008; Lee *et al.*, 2011] (3) Quality of rendering [Debevec *et al.*, 2008, Reinhard *et al.*, 2010, Kutulakos *et al.*, 2005] and (4) The method of adjustment task [Johnston *et al.*, 1994a and 1994b, McCrae *et al.*, 2013; Solteszova *et al.*, 2012, Bernhard *et al.*, 2016] that I adopted for my study.

## 2.1 Local Surface Geometry and Optical Information

The goal of constructing realistic water based images has long been pursued by the computer graphics community [Enright *et al.*, 2002, Peachy *et al.*, 1986, Foster *et al.*, 1995].

Many visual cues such as texture, shading, binocular disparity and other computer graphics effects are useful in three-dimensional shape reconstruction. Todd *et al.*, [2014] suggests that both position and surface orientation influence image intensity under both homogenous and non-homogenous illumination conditions. Participants estimated tilt and slant angles using a gauge figure task that measured observer's perception of local surface orientation on the depicted surfaces of translucent objects. The results clearly showed that (i) probe regions of similar orientations and positions can have large differences in image intensity (as shown in Fig 2.1) and (ii) for the given sets of stimuli, plausible light reflectance combined with any possible homogenous illumination could lead to ambiguous perceptions for the observers to estimate tilt and slant angles.

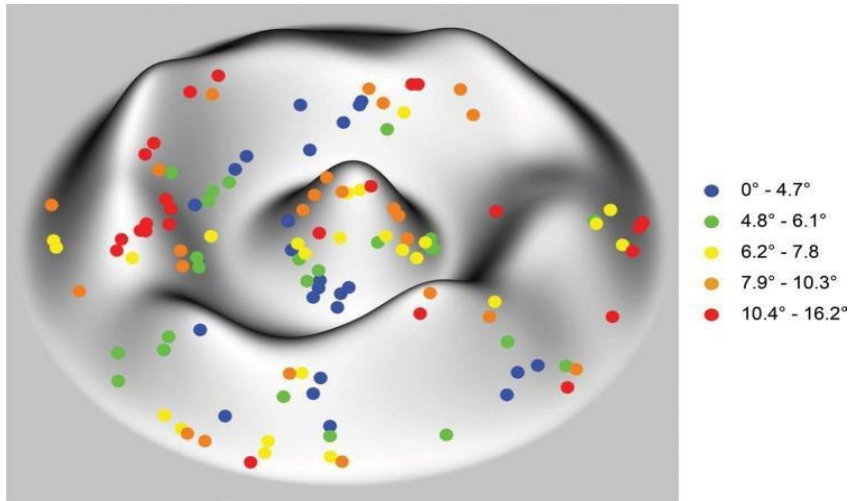


Fig: 2.1 Color-coded angular errors for surface shape estimation of a Lambertian surface with homogenous illumination. The red dots represent the highest marked errors and blue being lowest. [Todd *et al.*, 2014].

A similar gauge figure task was used by Fleming *et al.*, [2004] to investigate the perceived shape of perfectly mirrored surfaces in stationary images under uniform reflectance as shown in Fig 2.2. They reported that orientation fields are necessary for the perception of 3-D shapes and such fields remain invariant with respect to the change in specular location. Subjects were presented with a distorted reflection of a scene, and yet somehow were able to interpret the 3-D shape even in the presence of deceptive and unstable reflections using these warped patterns. This suggests that (i) specular reflections are sufficient cues for shape estimation and (ii) subjects need not construct a rich and accurate representation of the surrounding scene to recover shape from specular reflections.

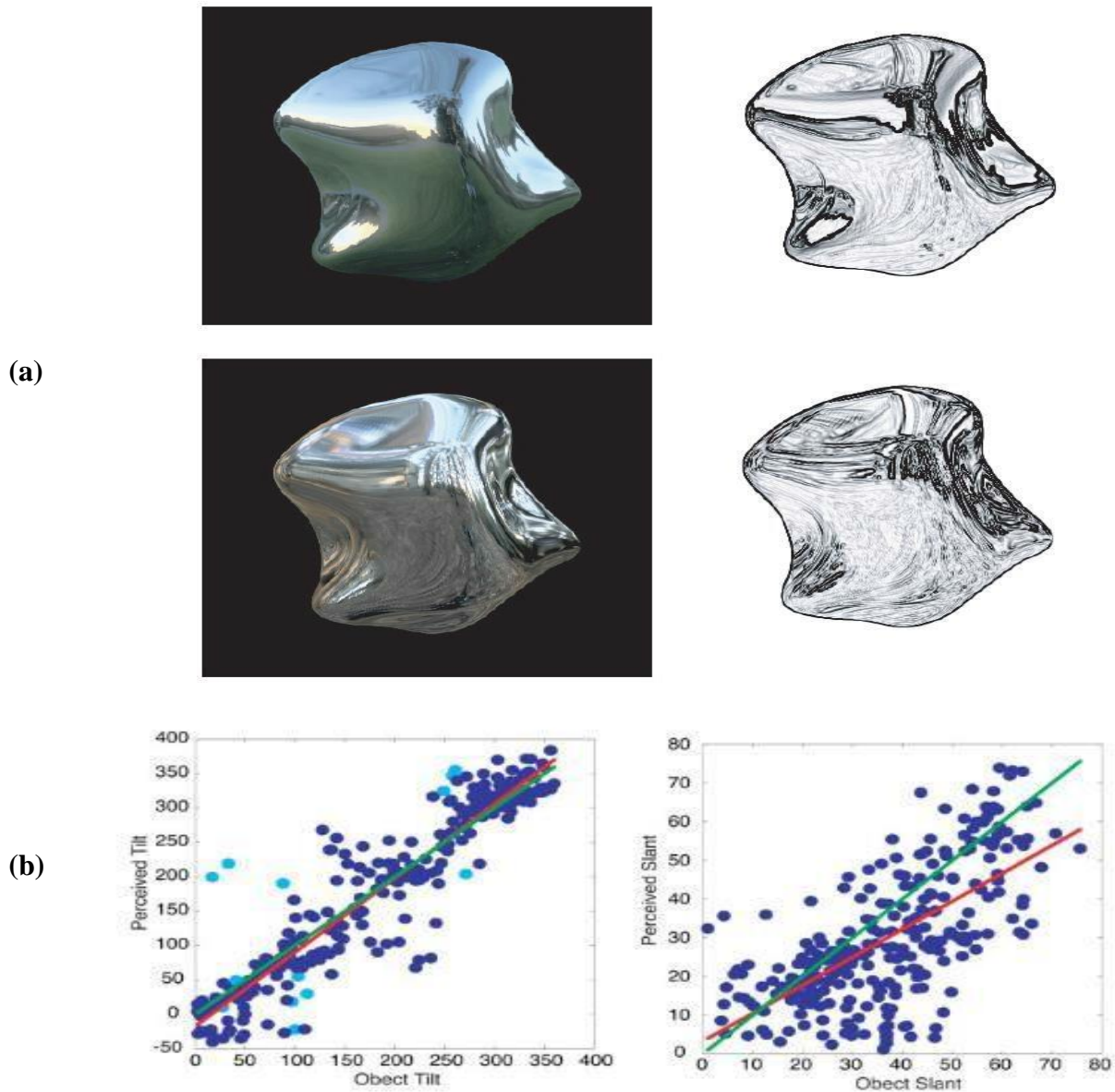


Fig: 2.2(a) The stimuli of specular mirror surfaces [Fleming *et al.*, 2004] showing stationary images with reflected environment and their respective edge-detection maps. (b) Plots pooled across two shapes, illuminations and subjects. Green line shows ideal performance, red line represents the best-fit of linear regression whereas Light blue dots indicate the tilt estimates for which slant is less than  $15^\circ$  (i.e., objective tilt is ill-defined).

More recently Kim *et al.*, [2016] generated images of deformed spherical objects using physically based rendering of refractive media and presented these either upright or rotated, as shown in Fig 2.3. The method to generate images of spherical objects used distortion field effects; which is a technique based on the magnification and minification of the patterns in the refracted structures of light to distort objects. The authors hypothesized that the orientation of the horizon could serve as a cue to distinguish between refractive (transparent) and reflective surfaces. The upright image (Figure 2.3(a)) produced a compelling percept of transparency (as though presented object was constructed entirely from ice or glass), whereas the rotated image (shown in Figure 2.3(b)) was perceived as more opaque and reflective.

Further, they investigated the effects of variation in refractive indices on the distortion field of light. Using the same fixed objects and light field method, the results indicated that increasing refractive index (i) increases the amplitude of the distortion field and (ii) increases the ratings of the perceived refractive index [Fleming *et al.*, 2011, Schluter *et al.*, 2014, Ueda *et al.*, 2015]. However, increasing the refractive index also reduces the critical angle for total internal reflection. This provides further important optical information which has a significant influence on subject's judgments of perceived shape, opacity, and refractive index. The image-inversion effect also suggests that the "global orientation" of photometric variations present in these distortions contributes to perceived transparency or degree of opacity.

This finding complements other studies that have identified illumination biases in the perception of other surface properties, including 3-D shape [Mamassian *et al.*, 2001]. This work suggests that distortion of texture or underlying geometry seen through refractive medium is an important cue to the shape of the surface. Another potential source of information to disambiguate surface shape could arise from the availability of multiple views of the surfaces.

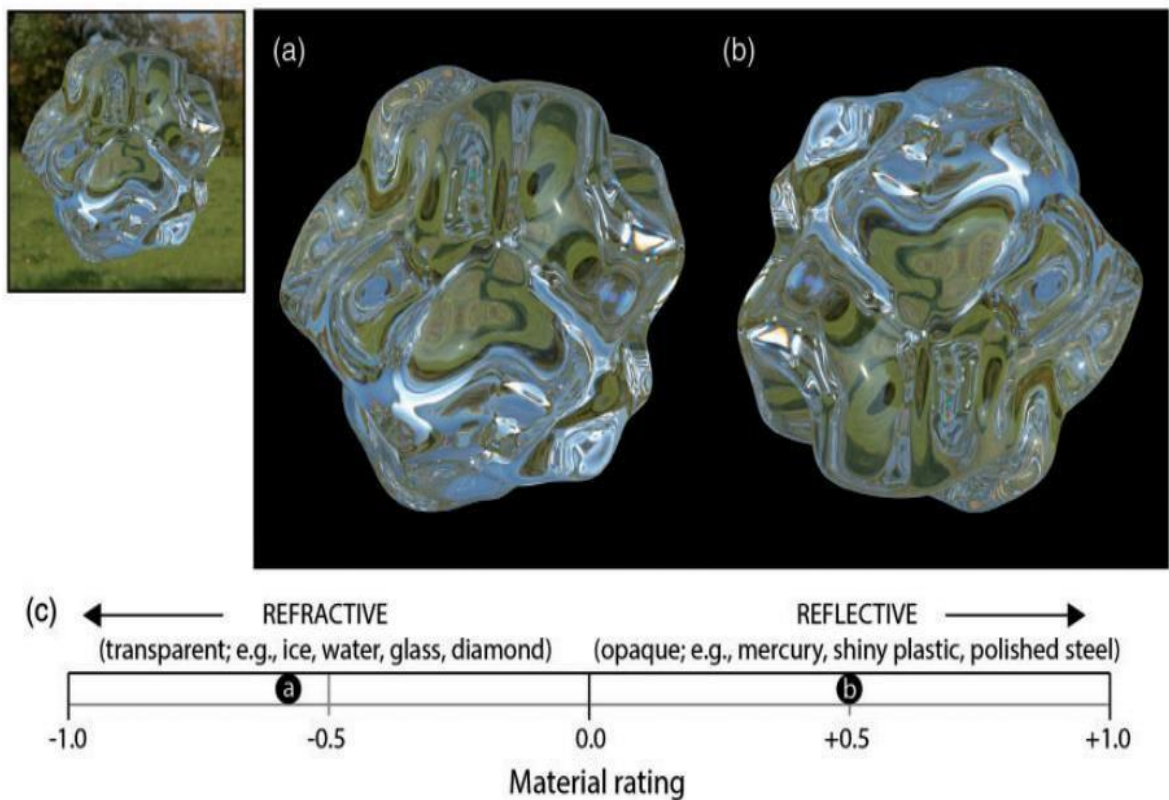


Fig: 2.3 Experiment images used by [Kim *et al.*, 2016]. Refractive rating shows the strength of opacity and degree of transparency.

Morris *et al.*, [2011] in their paper presented a computer vision system for reconstructing water surfaces using an indirect refractive stereo reconstruction method. The authors investigated whether two viewpoints are sufficient to recover the shape of transparent surfaces, even if the refractive index is unknown. They used two cameras under perspective projection to capture a single 3-D point and a normal on the surface. To map each point on the image plane to a known 3-D point that refracts to it, they computed pixel-to-point correspondence with a known checkered pattern underlying the water to measure the refractive disparity. They relied on a proposed method that measured the correspondences at  $t=0$  and used 2-D optical flow estimation to propagate these correspondences over range of pixels. Assuming that all the pixels have same refractive index value, they performed a one dimensional search through a reasonable index interval. For each hypothesized refractive index, they tried to reconstruct the scene for all pixels and frames by minimizing the refraction error due to refractive disparity in order to estimate 3-D position and normal of the surface point.

In their experiment, they suggested that as the liquid's surface height approaches the reference pattern at the bottom, refractive disparity diminishes. As ground truth data were not available in their scenario; they assessed their algorithm by applying it to the reconstruction of flat water whose height from the base of the tank varied. For each water height, they reconstructed point  $\mathbf{P}$  and a normal  $\mathbf{n}$  independently for each of the pixels in the 2 image planes.

They applied “stereo-matching” method for several dynamic water surfaces under variety of conditions as shown in Fig 2.4 below .The figures illustrates a ripple sequence initiated after single drop of water that caused layers of circular waves and a pouring sequence of water in an empty tank of known dimension. For such geometries of ambiguous refraction, their experimental results also suggested that stereo sequences could provide a generic way to estimate refractive indices. Their analysis also proposed that two surfaces with different refractive indices are not necessarily required to possess simple shape.

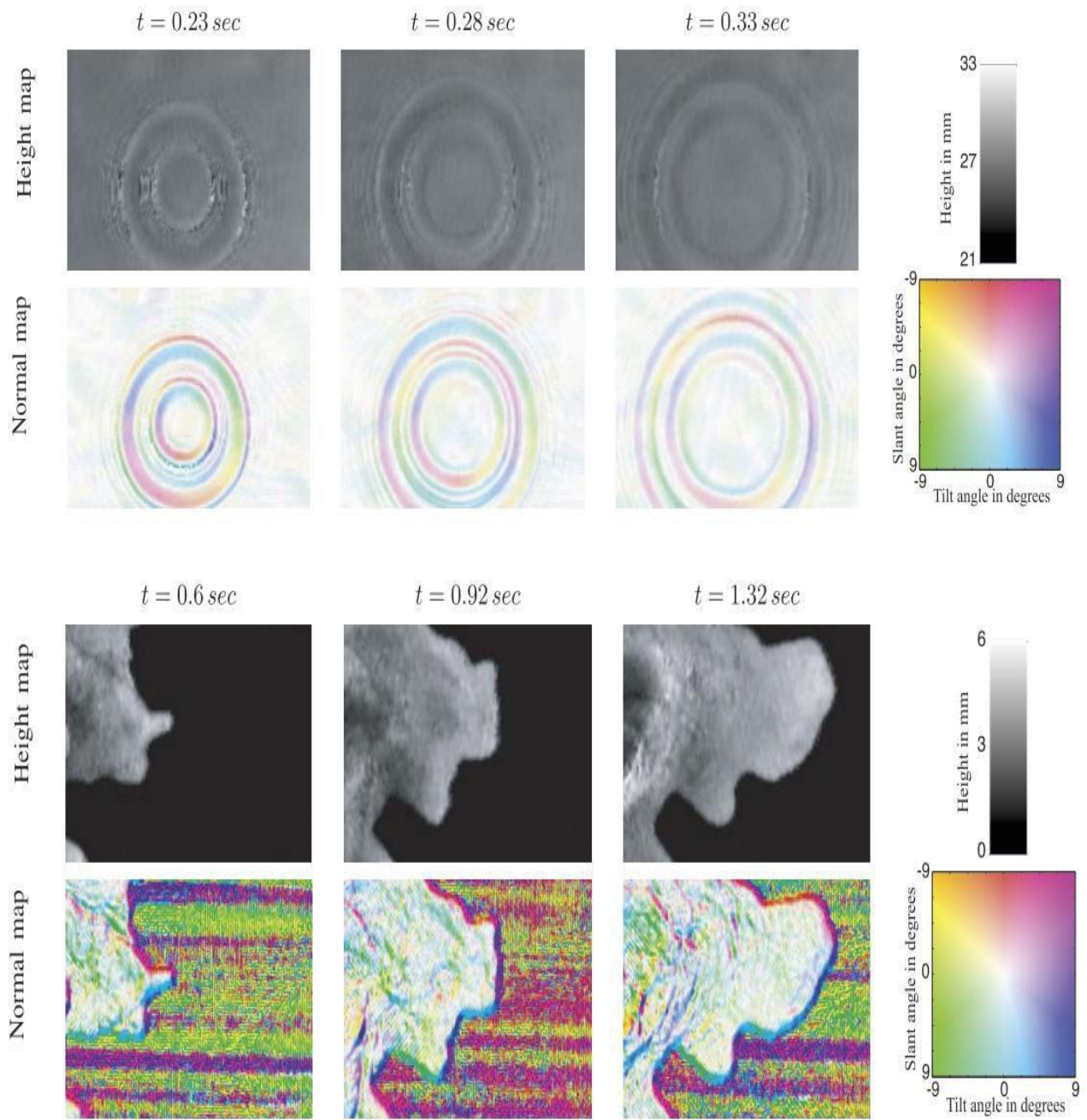


Fig: 2.4 represents Depth and Normal maps for three different time sequences of water-flow estimations to characterize shape distortion (pour and ripple generations respectively). [Morris *et al.*, 2011]

## 2.2 Stereoscopic and Non-Stereoscopic view

Several attempts have been made to reconstruct water surfaces using reflected light [Enright *et al.*, 2002, Morris *et al.*, 2011]. One approach uses traditional stereo image matching for Lambertian surfaces taken under natural lighting conditions [Shemdin 1990]. It is established by several well-known studies that stereopsis can provide reliable and consistent relative depth information required for surface orientation [Kersten *et al.*, 2006; Bridge *et al.*, 2008].

Lee *et al.*, [2011] found a consistent advantage for stereoscopic viewing over monoscopic viewing in people's ability to discriminate 3-D shapes for purely Lambertian reflectance and shiny surfaces.

On the contrary Pasqualotto *et al.*, [2009] investigated whether there was any benefit of stereo depth when 2-D cues could provide good information to support object's recognition. They tested the ability of subjects to recognize familiar objects in two different orientations. (a) Monoscopic condition, where stimuli were displayed as a flat 2-D image and (b) Stereoscopic condition, where objects were presented with stereoscopic depth. Their results suggested that when viewing angles changes were presented across 180° rotation (instead of 20° and 60°), stereo representations for similar objects increased the observer's response time.

They argued that the lack of explicit 3-D information in 2-D images may influence the recognition of familiar objects, when these objects are displayed on flat computer monitors.

### **2.3 Rendering approximations**

Rendering of synthetic objects of real-world scenes is an important application in computer graphics, particularly in architectural and visual effects domains [Debevec 1998]. Since this thesis presents synthetic photo-realistic water images to estimate shape change based on human visual judgement, fidelity in sampled image renders plays an integral part in the quality of the measurements. [Debevec *et al.*, 2008, Reinhard *et al.*, 2010]

Interactive computer graphics systems such as virtual reality or video games require that the graphics be updated in response to user interaction in a timely manner. Such rendering of static 3-D objects in a computer graphic world requires trade-offs with degree of realism in order to produce the graphics updates with acceptable latency and frame rate. Simplifications in rendering must be made while maintaining reasonable fidelity to support the accurate perception of surface properties such as texture, reflectance and transparency. To achieve un-biased rendering, various techniques have been introduced to overcome problems like large memory consumption, artifacts, inability to handle dynamic lighting, latency etc.

Debevec [2008] in his paper mapped synthetic objects with known reflectance model seamlessly into a real scene. He proposed an interesting solution to reduce the bottleneck problem of increased processing time required to render complex scenes. In his proposed method he segmented the areas of the scenes into 3 parts which were based on lighting models.

This segmentation optimized the regions which should be considered as part of the local scene and can safely be considered distant by identifying concentrated parts of indirect light. These localized light-independent parts of the scene reduced the processing time to render the image, however poses a limitation to produce high definition and realistically illuminated images.

## **2.4 Non-Linearity and bas-relief using Gauge Figure task**

The gauge figure adjustment method which is employed in my experiments estimates the polar coordinates of tilt (zeniths) and slant (azimuth) in 3-D space model (as shown in Fig 2.4). The elliptical gauge figure task [Koenderink *et al.*, 1992, Mamassian *et al.*, 1993, 1996] is one of the most popular and standard adjustment methods in psychophysical experimental settings to estimate local surface orientation [Fleming *et al.*, 2004, Todd *et al.*, 2014].

This technique localizes and intuitively estimates the perceived shapes of nearly all kinds and directly relates these to the precision with which observers make judgments of perceived surface normal. [Johnston *et al.*, 1994a and 1994b]

Although the gauge figure task is a common method used to study errors in surface perception [Solteszova *et al.*, 2012, McCrae *et al.*, 2013] in real time scenarios, the reliability of gauge alignment in mono and stereo display systems still presents challenging questions in terms of its accuracy [Bernhard *et al.*, 2016]. Bernhard concluded that the presence of gauge figure itself introduces bias in perceived shape

measurement of well-defined objects; however rendering the gauge figure in stereo settings produces more accurate slant estimates than mono-scopic rendering.

## **2.5 Summary**

The perception of transparent objects both in fluid and solid forms has received a great deal of consideration in recent times and impressive research has been conducted.

Despite this, the visual cues required to perform the task of shape reconstruction and complex phenomenon such as breaking waters [Morris *et al.*, 2011] in transparent media under distorted background environments are still not determined.

In light of this and to the best of my knowledge, no studies have considered local surface orientation for transparent material (such as water) using real time S3D gauge figure task presented in a 3-D environment. A key factor in visualizing a transparent object's shape is having sufficient geometric surface information. The fidelity in photo-realistic rendering and un-biased gauge figure measurements must deal with our accurate perceptual judgements in order to generate believable outcomes for shape reconstruction.

## **Chapter 3 Water Optics and 3-D simulation**

Water simulation and rendering has become an important problem due to water's ubiquitous nature and the growing use of computer-generated imagery in the field of digital cinema and print media. This challenge was faced by Pixar Animation in rendering realistic three dimensional water scenes in the making of the movie 'Finding Nemo'. Technical director Oren Jacob reported that their biggest challenge was that the team could never learn to master the vocabulary that describes all the nuances of 'how the water should look' until the end of the last shot of the movie. [Cohen.K, 2003]. This anecdote illustrates the importance of understanding how to evaluate the quality of water rendering and photo-realistic imaging which should provide a pleasing yet scientifically grounded simulation based on its intrinsic properties as a free flowing colorless liquid.

### **3.1 Physical and Optical Properties of Water**

Water exhibits unusual and unique properties in all its states. One can unconsciously notice this by experiencing its dynamics through big ocean waves or running water in a sink. Light plays an extremely important role in the perception of water properties like its degree of transparency, color and shape. Transparent objects in a virtual environment pose complex problems for interpretations of their shape because light paths are redirected at medium boundaries and light can be absorbed and reflected. The difficulty of this problem originates

from the viewpoint dependent appearance of such stimuli viewed in a 3-D environment.

In real world scenarios, when a light ray encounters a surface, one or more of the following three things occur, the light ray:

1. Reflects off the surface and travels off in a different direction.
2. Passes from one medium into the other and continue on a new, straight line path.
3. Is absorbed or scatter.

Water is a reflective surface. Ideally, for a flat still water surface, the angle of reflection should exactly be equal to the angle of incidence around a perfect imaginary straight line at a right angle to the reflective surface (this imaginary line is called ‘normal’). However, if there are ripples or waves in the water, the reflection becomes distorted.

The interaction of light with a water surface is described by Snell’s law (Eq: 3.1) which defines the behavior of light reflection and refraction at the interface between two media.

$$\mu_1 \sin (\theta_1) = \mu_2 \sin (\theta_3) \text{ ----- [Eq: 3.1]}$$

Where  $\mu_1$  is the refractive index of the first medium,  $\mu_2$  is the refractive index of the second and  $\theta_1$  and  $\theta_3$  are the incident and refracted angles. At the interface between water and air, there is a significant change in refractive index and light rays are noticeably refracted. Given that the index of refraction of air is 1 and that of water is 1.33, equation 3.1 can be

simplified for an air- water interface as Eq: 3.2. It is important to understand that the incident and refracted rays always lie in a plane, regardless of the direction of the surface normal. Therefore it is valid to visualize refraction at an interface in two dimensions (shown in Fig 3.1)

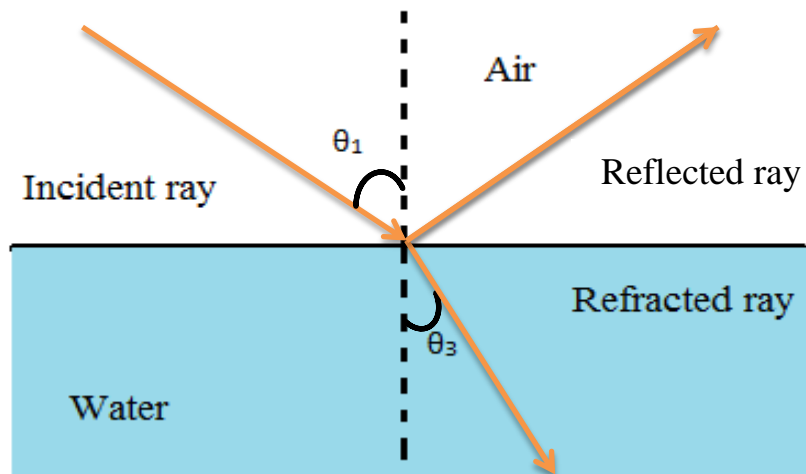


Fig: 3.1 Change in the direction of a light due to change in water density. [Adapted from Gettys.W.Edward *et al.*, 1989]

The incident angle ( $\theta_1$ ) and refraction angle ( $\theta_3$ ) describe the amount of light-bending which depends on indices of refraction of the 2 media and is quantitatively explained by Snell's Law.

Snell's law for an air-water interface can be written as:

$$\sin (\theta_1) = 1.33 \sin (\theta_3) \text{ ----- [Eq: 3.2]}$$

Based on this law, the refracted light crossing a planar specular surface has a point of intersection between the incoming ray of light, surface and normal at an angle from the surface normal of  $\theta_3 = \sin^{-1}(\mu_1/\mu_2 \cdot \sin \theta_1)$ .

### **3.2 Water Simulation in 3-D**

The physical properties that determine how water interacts with light provide the basics to simulate its motion and visual representation in 3-D. For the experiments, the visible shape of the water was computer rendered following 4 general considerations

- Surface is optically smooth hence there is no specular shading under uniform reflection (illuminated with sky-light).
- Computer generated images are stationary; hence cues from motion are not present.
- Water is transparent in nature; hence the underlying texture is a crucial input.
- Surface of water waves are assumed to be either flatly smooth or have ripples; hence the returning refraction of light greatly depends on the stationary position of the fluid.

### **3.3 Imaging of water surfaces**

I adapted the reconstruction method introduced by [Kutulakos *et al.*, 2005] where they used two spatially displaced camera views to capture the dynamics of water. Fig 3.2 below describes the predicted light path behavior when light interacts with the water where it is either emitted or scattered from a point under the water surface (i.e., 'the bottom' illustrated

at point 'd'). A ray of light from point d located on plane B under the water surface projects to the center of projection of the camera, represented at point 'C'. The distance between the camera center and point 'p' on the water surface where refraction of light from point 'd' towards 'c' occurs is to be determined. The angular displacement at 'p' results from Snell's law and thus is a non-linear phenomenon. To solve for the unknown variable 'z' (one side of deduced triangle); a trigonometric sine-ratio is applied:

$$\frac{\|p-c\|}{\sin(\theta_2-\beta)} = \frac{\|d-c\|}{\sin(\theta_1-\theta_2+\pi)} \dots\dots\dots [\text{Eq: 3.3}]$$

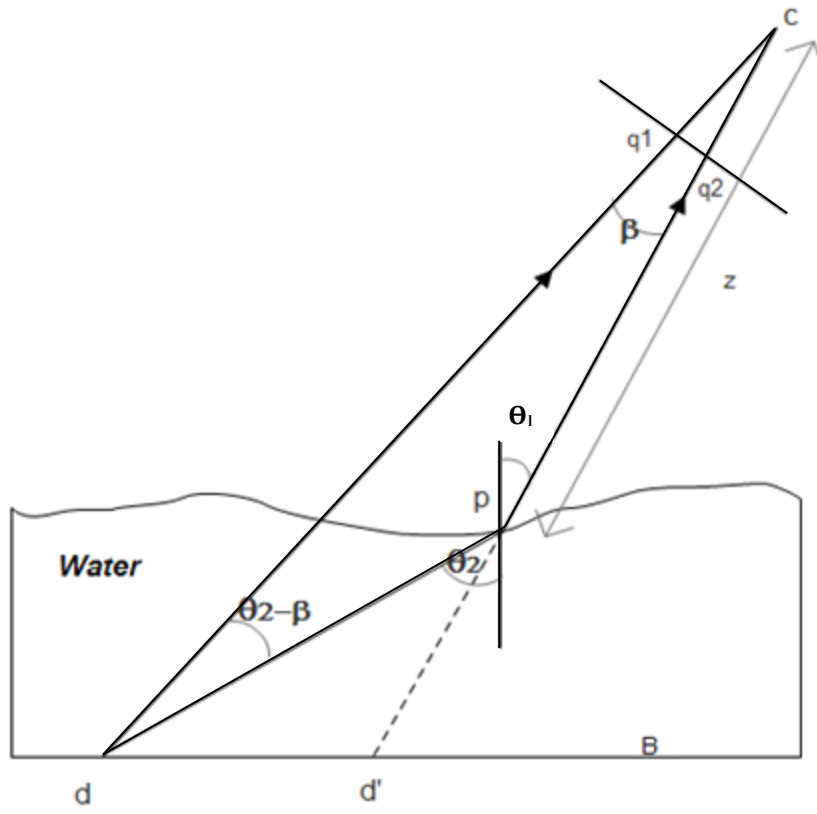


Fig: 3.2 Geometry of underwater refraction: Face-on-view to determine the  $z$  distance from the vertex of  $p$ . [Adapted from Morris 2004]

Suppose  $\|p-C\|$  equals  $\|z\|$ ,  $d$  is a known point lying on the base  $B$  and  $\|d-c\|$  is a known distance assuming there is no refraction when water is not present. The solution space is restricted to surface normal and depth due to the planarity constraint that restricts the refraction of the ray of light coming from ‘ $d$ ’ to image plane point ‘ $q$ ’. This distance can be optimized experimentally to deduce 1-D set of unique possible normals that forces discrete normal at  $p$  ( $d$ ) to lie on the plane defined by point ‘ $c$ ’ and ray through  $q_1$  and  $q_2$ . 3-D coordinates of the point on the pattern refract to pixels  $q_1$  and  $q_2$  on the camera plane representing pixel-to-point correspondence. Note that each discrete normal vector is associated with a unique depth value; therefore the determination of depth to find  $p$  is restricted to the normal surface that refracts the ray of incoming light.

### **3.4 Light-Path Triangulation**

I used “Light Path Triangulation” method to solve the problem of reconstructing water surfaces in stereo set up combined with the refraction over reflection technique [Morris *et al.*, 2005; Kutulakos *et al.*, 2007]. This method basically reconstructs a point through individual light paths (as a geometric constraint satisfaction problem) and generalizes the familiar idea of path triangulation to the case of indirect light projection.

A light-path is defined as the piece-wise linear path taken by a ray of light as it passes from a source, through the object and into the camera. Amongst several approaches to reconstruct refractive surfaces, light-path triangulation is often used because of its general applicability. [Chari *et al.*, 2013]

As the feature point's positions  $D1$  and  $D2$  (shown in Fig 3.3) are known [Morris *et al.*, 2004], given two views  $C1$  and  $C2$  of the scene; (each view with its own distinct surface normal), if light reaching the camera intersects with the water surface twice, we can restrict the problem to a finite set of possible shapes. This idea provides the mathematical basis for refractive light-path triangulation which is described below.

Consider a scene that is viewed from two known projective viewpoints ( $C1$  and  $C2$ ) and contains one object of unknown shape as shown in Fig 3.3. Suppose that two pixel points  $Q1$  and  $Q2$  are indirect projections of a 3-D surface point  $p$ , and there are identical light paths of unknown distances from  $p$  to  $C1$  and  $p$  to  $C2$ . Ray correspondence from feature points must be consistent with Snell's law that gives us two candidate normals for both the viewpoints. First normal suggests that point  $D1$  on the surface pattern refracts to  $C2$  via point  $Q2$ . The second normal enforces the similar condition to another feature point  $D2$  to refract at first projective viewpoint  $C1$ . Since each unknown point on the surface should have a unique normal; as a result, both normals should lie at same location ensuring a true surface point  $p$  for both refractions.

In addition to using a single projective view point (with the single camera), two projective viewpoints can be achieved by adding a second camera to obtain stereoscopic viewing condition. The two cameras must have parallel optical axes and be separated by a baseline  $L$  (as shown in Fig 3.3) which is perpendicular to the optical axes. Since it is required by the binocular stereo vision system to acquire two images of an object from different viewpoints, it is possible that the relative variables like  $z$ ,  $C1$ ,  $C2$  and angular displacements

can be triangulated at common surface point  $P$  using the method of refractive light path triangulation as discussed above.

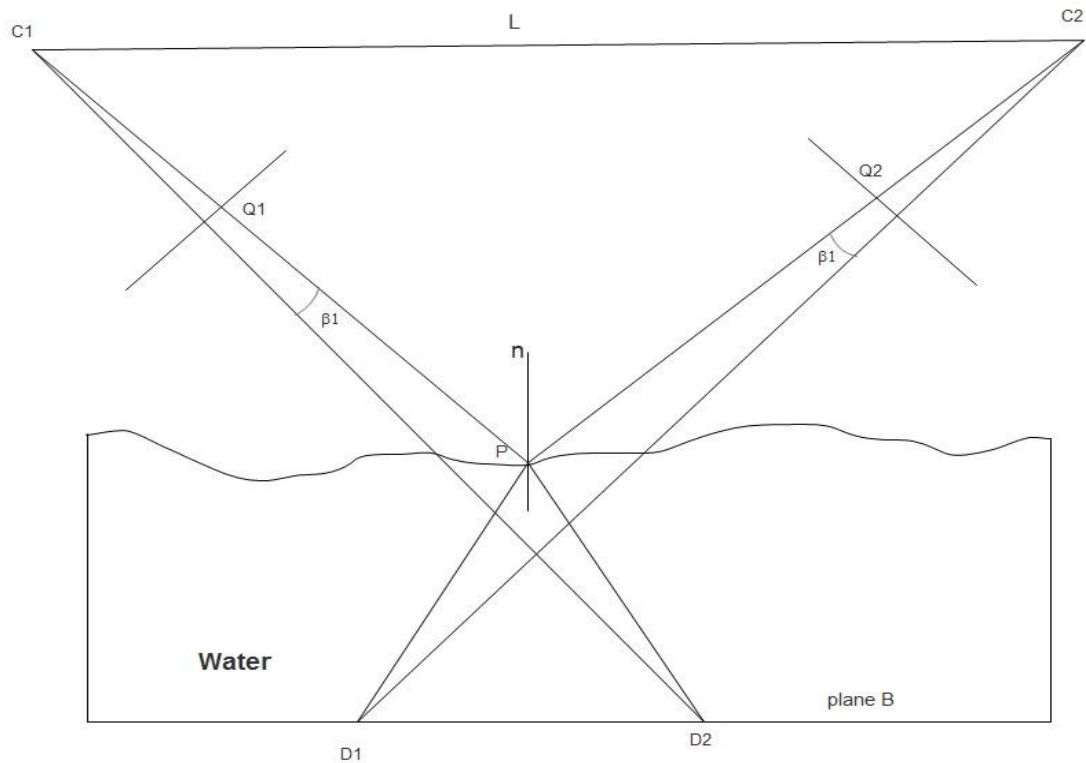


Fig: 3.3 Imaging Model:  $D1$  and  $D2$  are both refracted at point  $P$  and imaged in the two cameras at point  $C1$  and  $C2$  respectively. The rays triangulate in identical manner to intersect water surface and ensure common surface normal  $n$  for each unique surface point  $P$ . The approach can be used for Binocular Stereo Vision to reconstruct 3-D surface points in order to estimate object's shape. [Adapted from Morris 2004]

## Chapter 4 Experiment and Analysis

This chapter describes the method and procedure to test the theoretical predictions (discussed in Chapter 3) experimentally with human observers. I carried out the psychophysical experiments that enabled me to (i) obtain observer's estimate of the shape of refractive surfaces of water in 3-D virtual environment based on underlying textures (ii) determine which viewing condition improves the accuracy of perceived normal and if so, to what extent? and (iii) find about the specific points in the given scene that cause larger perceptual errors and why?

### 4.1 Methods

I designed a system that presents a stereoscopic-three-dimensional gauge 'method-of-adjustment' procedure to the subjects [Koenderink *et al.*, 1992, Mamassian *et al.*, 1993, 1996] with photo-realistic stimuli. It displayed pre-rendered stereoscopic images and a real-time S3D (Stereoscopic 3-D) shape probe simultaneously. The gauge pointer was used to indicate the perceived local normal direction at specified locations in a given stimulus. Fig 4.1 below illustrates the mathematical convention that I implemented in my study to establish the origin and axes of orientation for tilt and slant angles for gauge adjustments at several locations in given stimuli.

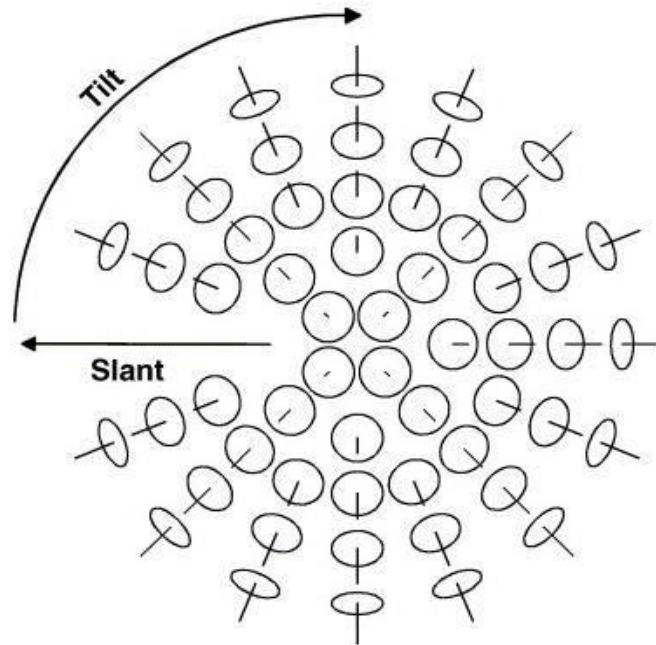


Fig: 4.1 A set of circular figures arranged on a sphere to illustrate the slant  $[0 < \Theta < 2\pi]$  and tilt  $[0 < \theta < \pi]$  components of surface orientation based on circular gauge probe. Note that the line at the center of each patch is aligned with the direction of the surface normal [Normal *et al.*, 2005].

#### 4.1.1 Apparatus

Stimuli were presented on a DELL 2670QM 3D LCD 17.3'' laptop screen with panel size of 38.2 cm  $\times$  21.5cm, pixel resolution of 1920  $\times$  1080 and a frame rate of 120Hz. The luminance of the white screen was 95 cd/m<sup>2</sup> per eye (through shutter glasses) that was measured by a Minolta LS-100 Luminance meter. NVidia 3-D shutter glasses were used to visualize stereoscopic 3-D images; the LCD shutters alternately blocked the right and left eye view and were synchronized with the alternation of the left and right images on the display. The glasses were worn in both stereoscopic and non-stereoscopic conditions. In order to perform the task with minimum interference and to establish a compelling fish tank

virtual environment, surrounds were kept dark. The head of the user was positioned 69.8 cm (nominal arm's length) from the screen such that the midpoint between the eyes lay on the perpendicular central axis of the screen (Fig: 4.2 show the physical set-up).

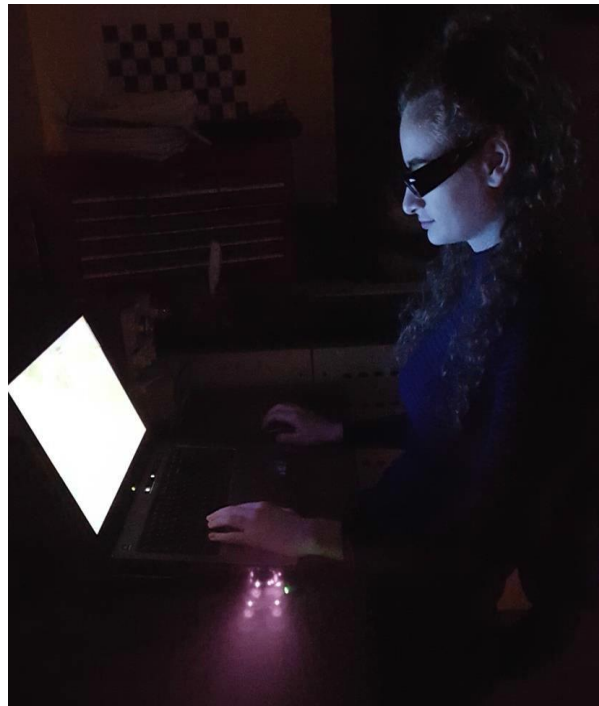


Fig: 4.2 Experimental set up with a subject performing the task of judging surface shape using mouse to adjust an overlaid 3D glyph indicating surface-normal. The viewing distance was about 69.8 cm.

#### **4.1.2 System's Software**

The script for the experimental code was developed on Visual Studio 2008 in C++. The images were rendered in Blender 2.75 [Flavell.L, 2010] with the ray tracing cycle engine. The rendering process involved many parameters controlling lighting, material and ray-tracing parameters. I list the important parameters which were involved during the image

rendering process. In modelling the scene, I adopted Preetham and Hosek models which eliminated the need of single point source lamp. The day-light model was illuminated by 'Sky texture' feature through Blender 'world shading'. [Preetham *et al.*, 2003].

The scene was constructed using a real time fluid simulation method. A water object was created using sub-division surface modifier to interpolate the geometry of wave surface shape. Each shape was rendered with 2 pours of liquid to cause ripples. The refractive index of water was kept at 1.33. I used an icosphere shape as a free falling mass to create wave texture for shape change over the water surface. In order to obtain still images (shown in Fig 4.3a), the rendering frame rate was kept as 24 fps Blender units with frame range of 1 to 250 to compromise between image quality and rendering speed per pixel. Over sampling was set to 16 to minimize rendering artifacts. Each normal map that stored 3 channel images (shown in Fig 4.3b) was generated in render mode while depth maps and actual RGB images were produced in Blender's cycle render mode. Two types of textures were used underwater. The regular base texture was built with an equal array size of diffuse tiles. The other noisy texture had similar material properties and was created as an unequal grid of asymmetric random blocks. For each object, I rendered three images of one stimulus from different viewing angles: left camera, center camera and right camera. They were identical cameras with optic axes offset of 65mm and parallel sensor widths of 32mm. The focal lengths of the cameras were 35mm whereas the field of view was 49.13°.

## **4.2 Subjects and experimental sessions**

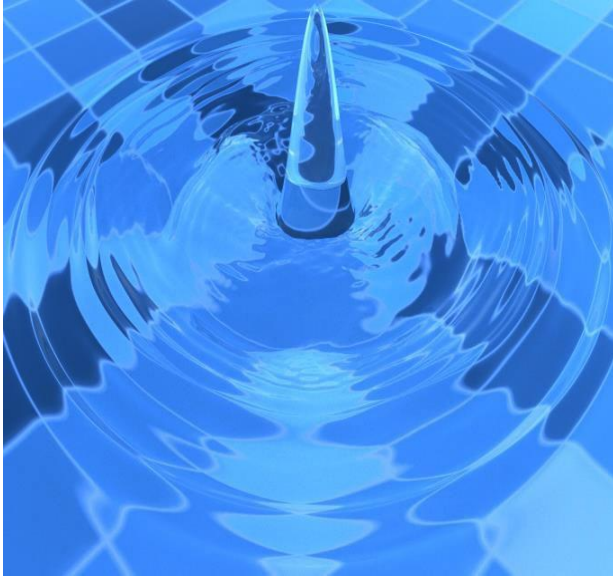
Eight graduate and undergraduate students from York University (four female and four

male, mean age of 24 years,  $SD = \pm 3.9$ ) participated in the experiment. They provided written informed consent and were compensated \$20 for their time. The experiment lasted an average duration of 2 hours including a 15-min practice session. Subjects were required to take a break of at least 4 hours between sessions or run the two sessions on separate days. All participants had normal or corrected-to-normal vision. They were screened for functional stereopsis using the graded circle test provided as part of the Stereo-Fly Test (Stereo-Optical Company, Inc. Chicago, USA). The eight participants in the study demonstrated the stereo acuity of at least 40 seconds of arc; a ninth subject did not achieve this inclusion criterion.

#### **4.2.1 Stimuli and Conditions**

The stimuli consisted of four static images (as shown in Fig 4.4a) having all combination of two wave shapes and two underlying textures (both regular and noisy one). There were two types of viewing conditions: One displayed the non-stereoscopic view from the center camera view to both eyes while the other provided a binocular view and appropriate stereoscopic view from left and right camera views. Therefore there were eight types of viewing conditions ( $4 \text{ objects} \times 2 \text{ views}$ ), and each image condition was tested in a separate block. All the images were binocularly viewed through shutter glasses. The program sampled 80 test points at arbitrary positions over the screen on each stimulus. The total number of measurements per subject was 640 ( $80 \times 4 \times 2$ ).

The sequential order of presented stimuli for eight tests was presented to each observer based on a ‘Balanced Latin Square method’ [Leonhard Euler 1707–1783].



Condition 1: Ripple shape and regular texture under non-stereoscopic condition



Condition 2: Ripple shape and noisy texture under non-stereoscopic condition

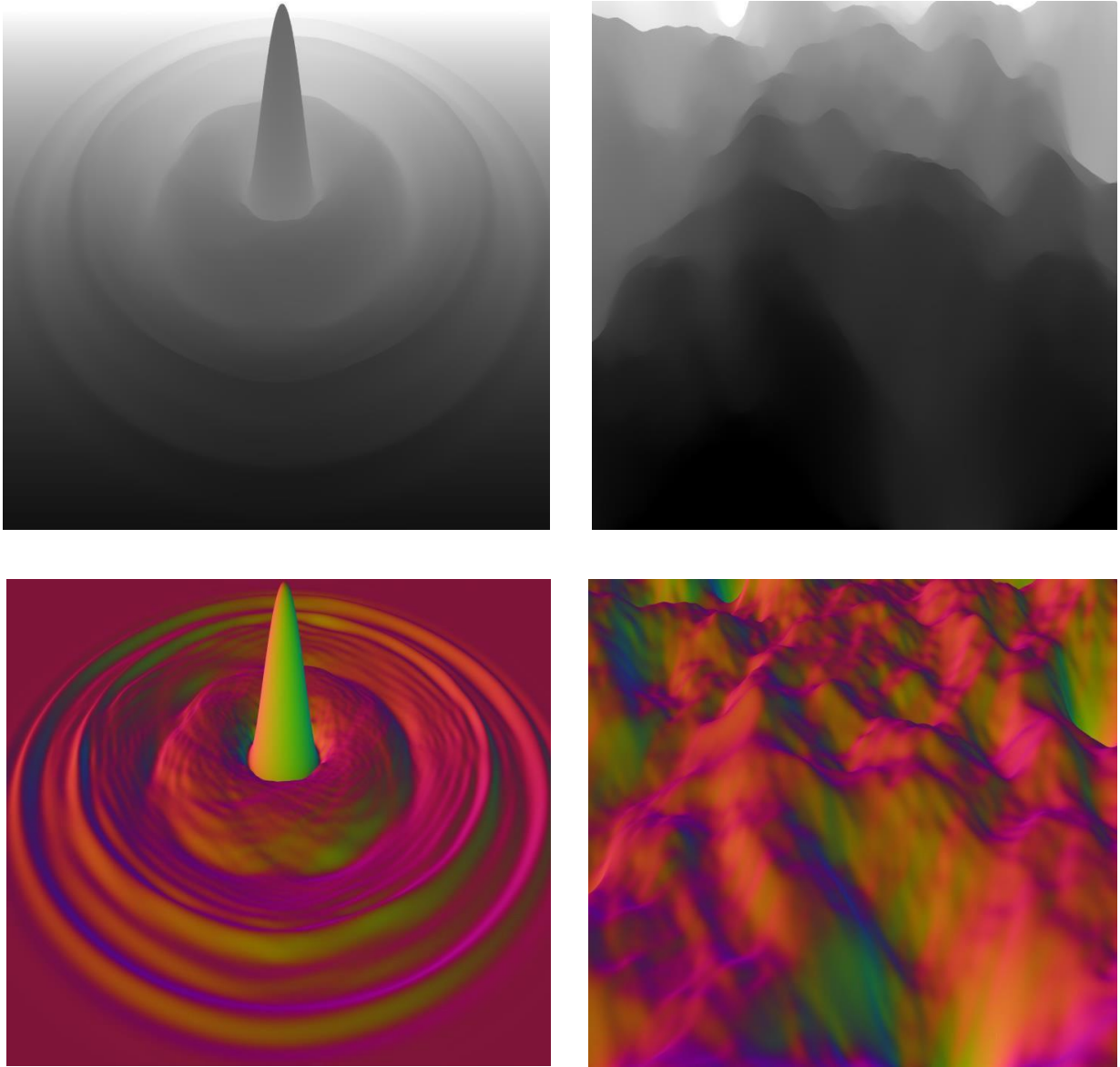


Condition 3: Wave shape and regular texture under non-stereoscopic condition



Condition 4: Wave shape and noisy texture under non-stereoscopic condition

4.3 (a) Stimuli objects of rendered water surface placed over regular and noisy base textures.



4.3 (b) Depth maps and Normal maps for corresponding stimuli in tangential space

Fig 4.3 above presents four stimuli objects used in the experiment with their respective depth and normal maps. Depth buffer in grey scale indicates the z-distance of the surfaces of the scene from camera view point [with pixel range of 0 ~ 255, zero being the farthest pixel location and 255 being the closest]. Normal maps represents RGB channel values that store normal vector information encoded through spatial dimensions of X,Y,Z coordinates.

### **4.2.2 Experiment Procedure**

Observers were asked to sit 69.8 cm away from the display with shutter glasses on as shown in Fig 4.1. Testing laboratory lights were turned off so that observer would get an impression of a 3-D interactive immersive environment with no stray light.

Prior to the actual experiments; participants were shown displays of a spherical shape object. Participants learnt to perform the task by running 40 test points over the surface of the sphere until they were fully accustomed to the task and the controls. The intent was to give subjects an understanding of the concept of normal direction and how to estimate normal direction using the gauge figure. Subjects were required to adjust the gauge direction to the normal direction at the designated point on the surface. When subject confirmed their estimation, the program calculated the angular difference between the estimated angle and ground truth. If the difference was less than a threshold of  $15^\circ$ , the gauge was set to the next position; otherwise, the program displayed a green color reference to show surface orientation. The subjects were required to adjust the gauge direction until the angular difference was less the threshold. The practice session lasted for about 10-20 minutes. After the practice, every subject was familiar with the task and how to adjust the gauge to indicate the perceived normal direction.

In the main experiment, separate blocks were presented to the subjects for each of the four stimuli under both stereoscopic and non-stereoscopic viewing conditions. They were required to adjust the gauge figure to be perpendicular to the surface at the given test point.

Once satisfied with their adjustment, they pressed the space button on the keyboard to confirm their decision and move on to the next position. The test points were presented in pseudo random order for each individual observer in order to avoid predictability. Although unlimited time was given to subjects to perform the task of estimating correct orientation of surface shape, I encouraged them to complete each session at a constant speed so that they should not spend undo time on a particular trial. It was noted that after processing the perceived judgements based on visual cues, observers took an average of 15 minutes per stimulus to adjust the gauge figure. During the experiment, all of the users reported that the given images produced clear impression of transparent water wave surfaces with pool tiles lying beneath. Figure 4.4 below depicts an observer performing the gauge adjustment to orientate the normal aligned with the surface shape.



Fig 4.4 Screen shot of gauge figure. Subject adjusting the overlaid probe at the stimuli surface

### 4.3 Results and discussion

#### 4.3.1 How well do humans perceive the shape of transparent objects?

I predicted that people should be able to perceive the surface slants and curvatures of water shape from both stereo and non-stereoscopic views but shape from stereoscopic view would produce more accurate results than non-stereoscopic conditions.

The perceptual errors were measured as the angular displacement between the estimated normal directions and their corresponding ground truths based on the following equation which represents the dot products between two vectors in 3-D space

$$\text{Angular error} = \cos^{-1}(n_{es} \cdot n_{gt}) \dots\dots\dots [\text{Eq: 5.1}]$$

Where  $n_{es}$ ,  $n_{gt}$  are the estimated normal direction and ground truth of normal direction, respectively.

Average errors for each subject and object under both viewing conditions were calculated and used to describe the accuracy of perceived surface normal direction. I used 95% confidence intervals to describe the confidence in the perceived average error. Figure 4.5 shows average errors and confidence intervals for each subject and viewing condition. I found that subjects could perceive the normal directions of a transparent water surface consistently: average error across all trials was  $24.6^\circ$  which was slightly larger error compared to  $22.7^\circ$  from the previous study [Chen and Allison. 2013]

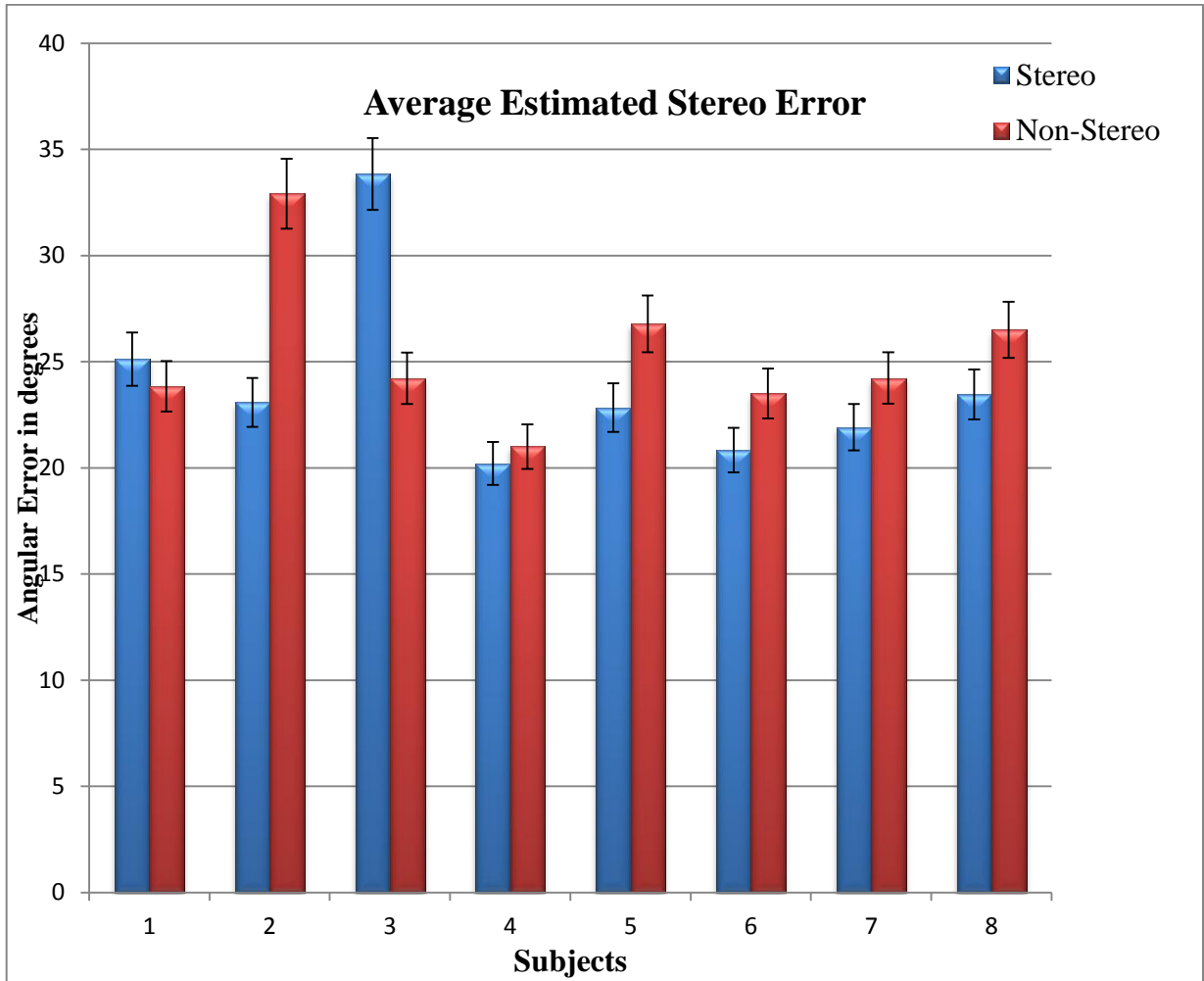


Fig: 4.5 Average estimation errors and confidence intervals (95%) for each subject and viewing condition

to perceive shape for thick glass transparent objects.

Moreover perceived errors from stereoscopic view were smaller than non-stereoscopic view for all shapes and underlying textures ( $23.9^\circ$  versus  $25.3^\circ$ ) but the group difference was not significant (paired  $t(7) = -0.7$ ,  $p=0.47$ ). Although two out of eight subjects were more accurate under non-stereoscopic viewing than stereoscopic viewing condition, there were individual differences. For example the average stereoscopic error of subject number three was larger than average non-stereoscopic error of subject number two and vice versa. There could be at least two causes for inter-individual differences. First, subjects may have different visual abilities to perceive the shapes of transparent objects. Second, subjects may have different abilities to set the gauge to the desired slant and tilt directions even though they were given ample amount of time to practice with the GUI system.

The gauge figure task assumed that subjects could accurately perceive the normal direction of the displayed gauge and could precisely adjust the gauge to their perceived normal directions. Actually, both assumptions might be invalid. I measured the performance of the subject's adjustment capabilities by estimating the shape-stereo error of basic sphere. Since the subjects already know the shape of the object, the task assessed the precision of the adjustments. As in the sphere case (average stereo error  $=7.968^\circ$ ) was much smaller than in the experimental trial, the error in the experimental conditions is most likely perceptual.

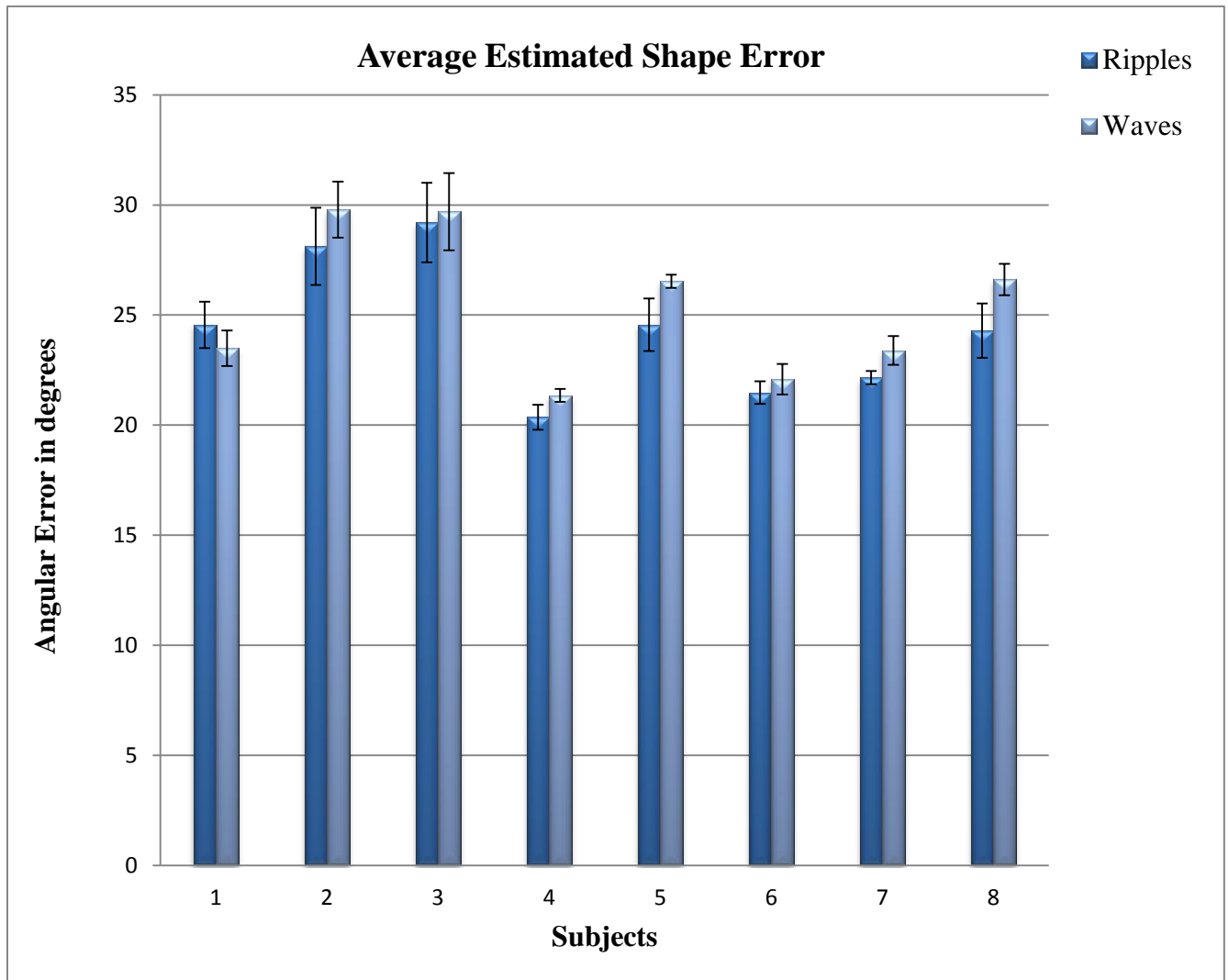


Fig 4.6 Average estimation errors and confidence intervals (95%) for each shape by each subject

Fig 4.6 shows average errors and confidence intervals for each subject and shape of the transparent water surfaces. As expected, the normal directions were significantly more accurate for the perceived ripple shape than complex mixed waves. (paired  $t(7) = -2.7$ ,  $p = 0.028$ ).

#### **4.3.2 Do cues from textures provide useful information to perceive shape?**

Perception of the 3-D shape of a smoothly or sharply curving transparent surface can be facilitated or impeded by the use of different surface texture patterns present in the background environment. Appropriate textures might facilitate accurate perception of surface shape in renderings of data. Fig 4.7 shows that overall, subjects seem to do somewhat better to perceive shape with regular texture than with the noisy ones under both viewing conditions. The average perceived error for regular or geometrically identical texture pattern was  $23.92^\circ$  and significantly smaller than perceived angular error in the case of noisy texture pattern ( $25.46^\circ$ , paired  $t(7) = -3.3$ ,  $p = 0.012$ ). Based on the reduced error in case of regular texture pattern underlying transparent water surface, I could speculate that symmetry that exists in the texture size and predictable repetition in its geometrical shape can somewhat improve our perceptual understanding of ambiguous or unknown transparent shapes presented in its foreground.

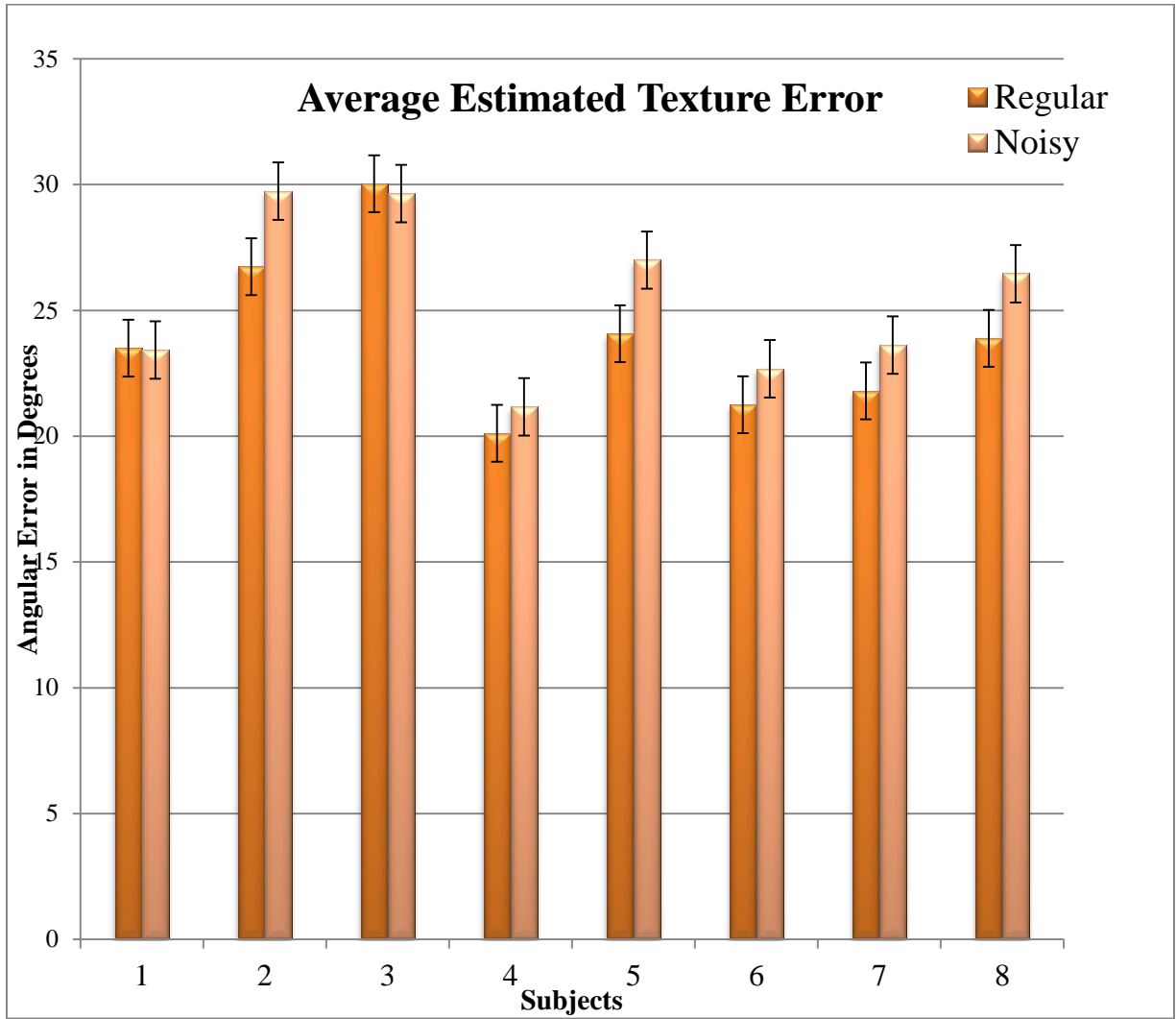


Fig 4.7 Average estimation errors and confidence intervals (95%) for each texture

### **4.3.3 Which areas had larger perceptual errors and why?**

Since the experiment densely sampled test points on various locations on the surface of the transparent objects, I was able to successfully analyze the pattern of errors over the scene to determine if the errors were localized on few important areas of the stimuli. For each experimental condition, I sorted the estimation error in terms of frequency of occurrences. To visualize the error distribution, I selected the surface locations with the largest errors out of 80 test points for each observer (shown in Fig 4.8a and 4.8b) and marked them as perceptually challenging surface points in both stimuli conditions. Figure 4.8a shows that the most recurring error of  $65.41^\circ$  was localized in area of the scene at the ridge of the curve in case of first shape (marked with a yellow dot). It can be observed that highest error of  $123.01^\circ$  was perceived at the point where there is no sufficient information from the underlying texture and shape change is also insignificant.

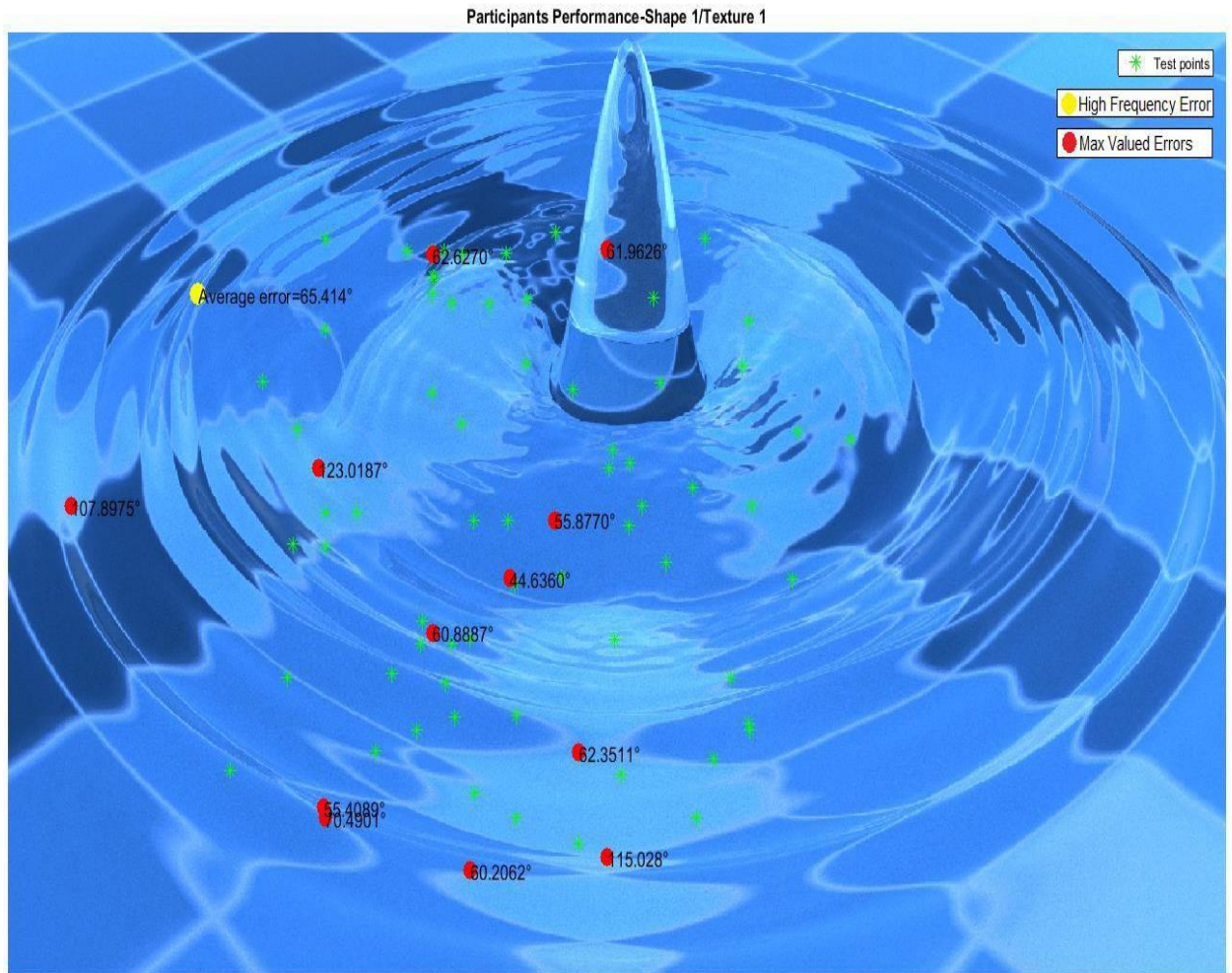


Fig 4.8(a) Largest and high frequency sorted errors of ripple shape under regular texture pattern

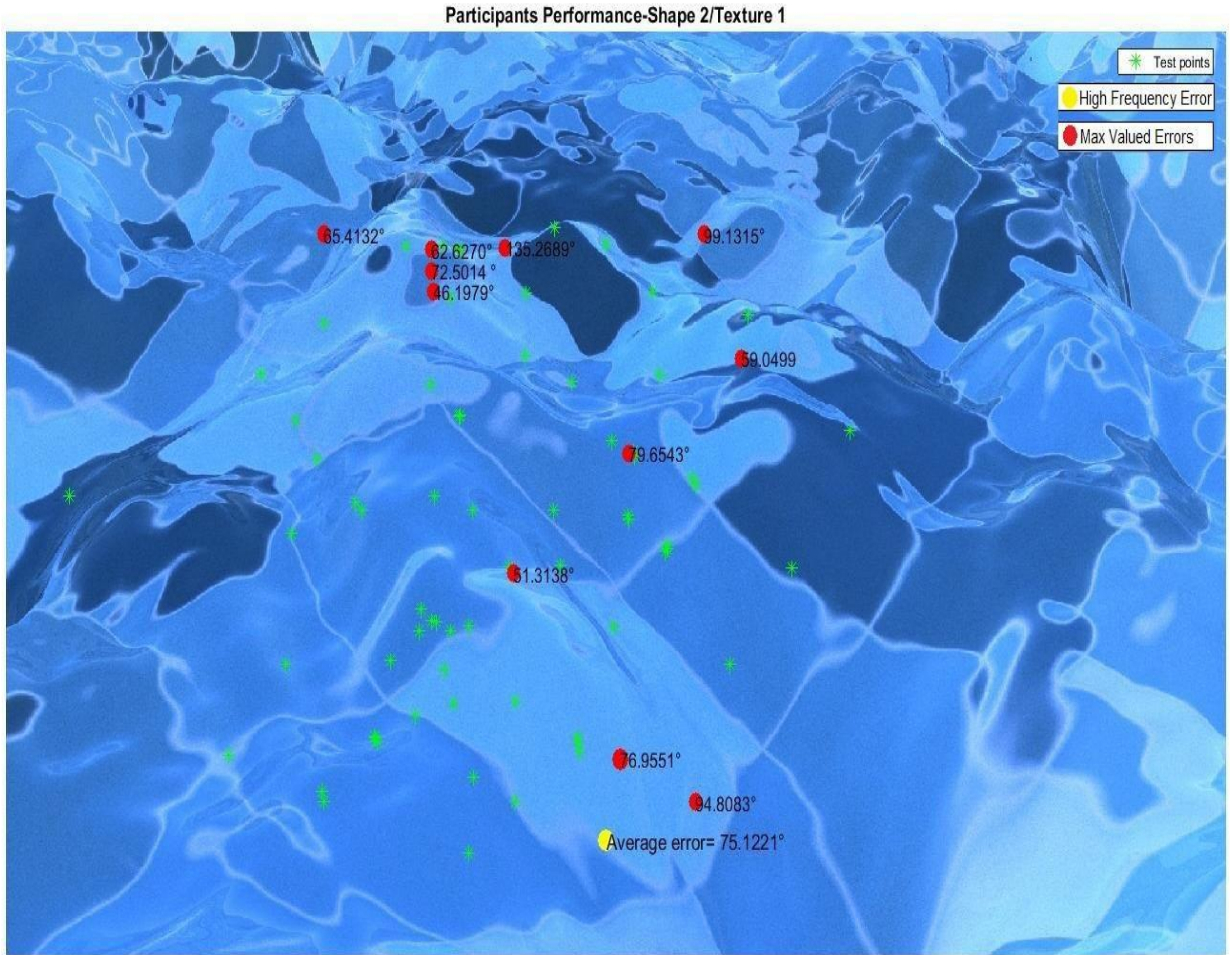


Fig 4.8(b) Largest and high frequency sorted errors of wave shape under regular texture pattern

#### **4.4 Discussion**

Transparency is an important aspect of material appearance. To some extent, humans are able to consistently estimate transparency and its shape across different lighting conditions and backgrounds. However for transparent objects, there is a large variation in shape and types of materials like glass, plastics, water or other liquids hence; these objects appear to present ambiguous shapes when placed in different types of environments. Also a transparent object can have all kinds of colors, translucency and refraction and/or reflection properties. In my experiment, I only explored one particular transparent liquid type with relatively simple surfaces rendered under day-light setting. However, I believe that they are sufficient for the claims that I presented in this thesis. As expected for all four experimental stimuli, surface perception was sensitive to changes in the viewing condition. The stimuli objects used in the experiments can also be modified to various other potential shapes. Previous work and our theoretical analysis suggests that orientation information, underlying textures cues and viewing conditions play a determining role in shape judgement and surface reconstruction, and is relatively invariant across surround environments. Thus I assume that similar results would be obtained with different transparent and refractive materials and people should be able to consistently perceive desired surface shapes of other transparent objects based on similar method proposed in this thesis. Since the light path of refractive objects has similar properties to that of reflective objects, I predict that visual information such as texture orientation, edges and type of material can provide visual cues for the surface orientation and reconstruction of transparent objects.

## **4.5 Limitations**

### **4.5.1 Differences of perception from stereoscopic images and real world objects**

I used realistic computer generated graphics to approximate the view of real world water surfaces. The scenes reflect realism but still fell short of fully modelled environment and high quality rendering. As with all computer graphics representation, they also fell short of a perfect picture quality. There are two main reasons for the difference between the perception from stereoscopic images and the perception from a real world 3D object. First, stereoscopic images provide just a single binocular view of a real object. When people view an object from stereoscopic images, they can obtain the depth information from disparities between the left and right image, however this information is fixed when a viewer changes head position, distance from the object or the convergence of eyes. On the contrary, when people view a real object to perceive its shape, they may move their heads to obtain additional information from motion parallax and accommodation changes when one fixates at different viewing distances. Second, synthetic objects lose or change visual information in the rendering, simulating and modeling process. In short, computer imitations cannot fully replace experiments on real world objects. As a result, decision to use such stimuli in an experiment is a trade-off between reality and parametric control of the image generation processes presented through virtual reality.

### **4.5.2 Different transparent objects with range of texture maps**

The images I used in my experiments are only water based and only reflected light once. Although the stimuli represent several important natural phenomenon, many transparent

objects violate these constraints. This experiment used only two background texture maps warped with two shapes, which might not be able to represent the generality of application. Also the two water wave surfaces rendered might not be able to fully cover the diversity of natural scenes. While empirical evidence from previous work [Flemming *et al.*, 2004] and the literature review discussed in section 2.1 demonstrate that shape from reflective/refractive objects depends on orientation map rather than direction information from scene, it is still essential to test subjects within different natural scenes to test the generality of findings. Also I found that particular areas of objects were difficult to perceive. It would be interesting to investigate what types of objects with particular shapes are most challenging for shape perception.

### **4.5.3 Gauge probe task control**

The gauge probe adjustment method may be subject to perceptual bias making it difficult to distinguish errors of misperceiving the orientation of a surface from precise control in the orientation of gauge in 3-D [Cole.F *et al.*, 2009]. As discussed in section 2.4, the gauge orientation task suffered from several limitations in my experiments which could be minimized by proper practice, but cannot be completely eliminated. Finally, I used only a few test points which were recorded over the experimental stimuli for each gauge setting to make this approach practical. Hence the study limits the possibility to cover all parts of the scene to recover surface where interesting points could be more disposed to investigate human shape judgment.

## **5 Conclusion and Future Work**

In this thesis, I presented an experimental system based on Chen and Allison [2013] for estimating and analyzing human visual perception of surface shapes of transparent objects, particularly water. This system utilized pre-rendered photo-realistic stereoscopic images and a real-time gauge adjustment method to measure the perceived water surface shape at arbitrary locations in still images. This study contributed to the areas of human visual perception and perceptually guided rendering by developing a system that rendered shapes of volume of water in 3-D virtual space. These shapes were based on locally parameterized geometric solution using an ortho-stereo set-up, characterized by the physics of light path transport phenomenon. The method used for experimental analysis combined 3-D geometry information from the depth maps and normal maps of rendered scenes. Through the experiments, I tested a novel hypothesis that stereopsis can improve the perceptual accuracy of surface shape estimates when objects are rendered in a 3-D scene. However, the hypothesis was not supported as the group difference between stereo and non-stereoscopic viewing conditions was not statistically significant.

The results confirmed my prediction that people tend to interpolate geometric orientations from object's dominant boundaries and neighboring areas. I also found that regularity in background texture map provides useful visual information to facilitate people's perceptual judgement to consistently perceive shapes of water surface. Based on the analysis, I also conclude that the larger errors were located in certain areas of the given surface, such as ambiguous ridges and plain textures.

These findings collectively contribute to an understanding of human shape perception and the role of textures and viewing conditions involved in this process.

## **5.1 Future Work**

There are various possibilities and opportunities to improve and extend the study as future work.

A perhaps more immediate direction for future work is the investigation of the effect of texture orientation on surface shape judgments when the texture pattern is defined by surface relief rather than surface luminance.

Currently, the system only tests water as one of the transparent liquids. From computer vision perspective, the investigation of general transparent fluids that are used in everyday life for example honey, liquid soaps etc and other thick glass or plastic made objects could also be useful to explore and yield interesting results for the recovery of surface shape. Computer graphics approaches, describing the forward problem of light transport can be used to obtain additional insight to recover scene parameters. Besides local surface geometric information like orientation or/and texture maps, I suggest that additional visual cues such as shading, caustics, highlights and translucent properties will provide useful information to viewers for shape judgement of objects as mentioned. Such objects could be tested as objects of interest from scientific point of view in areas as diverse as oceanography, applied optics and experimental perception .I hope to investigate other potential applications that might be useful to the community.

## Bibliography

- BERNHARD, M., WALDNER, M., PLANK,P., SOLTESZOVA, V., AND VIOLA, I. 2016. The Accuracy of Gauge-Figure Tasks in Monoscopic and Stereo Displays *IEEE Computer Graphic Appl.* 36(4):56-66.
- CHARI, V., AND STURM, P. 2013. A Theory of Refractive Photo-Light-Path Triangulation. *The IEEE Conference proceedings on Computer Vision and Pattern Recognition (CVPR)*, 2013, pp. 1438-1445
- CHEN, J AND ALLISON, R. 2013. Shape perception of thin transparent objects with stereoscopic viewing. *ACM Trans. Appl. Percept.* 10, 3, Article 15 (August 2013)
- COHEN .K. June 2003.Technology, Animation World, VFXWorld  
<http://www.awn.com/animationworld/finding-right-cg-water-and-fish-nemo>
- COLE, F., S,KEVIN,. DECARLO,D., FINKELSTEIN ,A., FUNKHOUSER,T., RUSINKIEWICZ, S., SINGH,M., August 2009.How well do line drawings depict shape? . *ACM Trans. Graph.* 28, 3, Article 28 (July 2009).
- DEBEVEC, P. 2008. Rendering synthetic objects into real scenes: bridging traditional and image-based graphics with global illumination and high dynamic range photography. In *ACM SIGGRAPH 2008 classes (SIGGRAPH '08)*. *ACM*, Article 32, 10
- DOUGLAS, E., STEPHEN, M., AND RONALD. 2002. Animation and rendering of complex water surfaces. In *Proceedings of the 29th annual conference on Computer graphics and interactive techniques (SIGGRAPH '02)*. *ACM* , 736-744.

ENRIGHT, D., MARSCHNER, S., AND FEDKIW, R 2002. Animation and rendering of complex water surfaces. In *Proceedings of the 29th annual conference on Computer graphics and interactive techniques (SIGGRAPH '02)*.ACM, NewYork, 736-744.

ENRIGHT,D., FEDKIW,R., FERZIGER,J., AND MITCHELL, I. 2002 .A hybrid particle level set method for improved interface capturing. In *Proceedings of SIGGRAPH 2002, ACM Press / ACM SIGGRAPH, 2002*.

EZRA, M. BEN AND NAYAR, S. K. 2003 .What does motion reveal about transparency. In Proc. *International Conference on Computer Vision (ICCV)*, Nice, pp. 1025-1032

FLEMING, R., TORRALBA, A., AND ADELSON, E. 2004. Specular reflections and the perception of shape. *Journal of Vision* 4(9), 798-82

FLEMING, R.W., JÄKEL.,F AND MALONEY.,L 2011.Visual Perception of Thick Transparent Materials. *Psychological Science Online First*, published on May 19, 2011.

FOSTER, N., AND METAXAS, D. 1996. Realistic Animation of Liquids. In *Graphical models and image processing*, Volume 58, Issue 5, September 1996, 471-483

GETTYS.W.EDWARDS, KELLER. FREDERICK J., AND SKOVE. MALCOLM J. 1989.*Physics, classical and modern*. New York : McGraw-Hill, 1989. ISBN:0070335230

JESCHKE, S., WIMMER, M., AND PURGATHOFER, W. 2005. Image-based Representations for Accelerated Rendering of Complex Scenes .EUROGRAPHICS 2005 STAR – *State of The Art Report*. Institute of Computer Graphics and Algorithms, Vienna University of Technology, Austria

- KIM, J., AND MARLOW, P.J. September-October 2016. Turning the World Upside Down to Understand Perceived Transparency. *i Perception*, 1–5. [ipe.sagepub.com](http://ipe.sagepub.com).
- KUTULAKOS, K. N AND STAGER, E. 2005 .A Theory of Refractive and Specular 3D Shape by Light-Path Triangulation. *In Proceedings of the Tenth IEEE International Conference on Computer Vision (ICCV'05)*.
- LANGER, M.S., BÜLTHOFF, H.H. 2000. Measuring Visual Shape using Computer Graphics Psychophysics. *Rendering Techniques 2000: Proceedings of the Eurographics Workshop in Brno, Czech Republic, June 26–28, 2000*. Springer Science & Business Media, 2013.
- LANG, M., ALEXANDER, H., OLIVER, W., STEVEN, P., ALJOSCHA, S., and MARKUS, G. 2010. Nonlinear disparity mapping for stereoscopic 3D. *ACM Trans. Graph.* 29, 4, Article 75 (July 2010)
- MICHAEL, B., GUIFANG, L., AND ERIC VAN, S. 2010. *Optical Properties of Materials, Nonlinear Optics, Quantum Optics*. Handbook of Optics, Third Edition, Volume IV: McGraw Hill Publishers. ISBN: 978-0-07-162929-4
- MIYAZAKI, D AND IKEUCHI, K. Nov 2007. Shape Estimation of Transparent Objects by Using Inverse Polarization Ray Tracing. *IEEE Transactions on Pattern Analysis and Machine Intelligence*. Volume: 29, Issue: 11.
- MORRIS, N.J. 2004. Image-based Water Surface Reconstruction with Refractive Stereo. Master's Thesis. University of Toronto.
- MORRIS, N.J AND KUTULAKOS, K. N. 2011. Dynamic Refraction Stereo. *IEEE transaction on Pattern Analysis and Machine Intelligence*, Vol. 33, No. 8

MURASE, H. 1990. Shape reconstruction of an undulating transparent object. *In Proc. IEEE Intl. Conf. Computer Vision*, 313–317.

NORMAN, F., TODD, J. T., NORMAN, H.F., CLAYTON, A.M., MCBRIDE, T.R. November 2005. Visual discrimination of local surface structure: Slant, tilt, and curvedness. *Published in Vision Research* 46 (2006) 1057–1069.

PASQUALOTTO, A AND HAYWARD, W.G. October 2009. A stereo disadvantage for recognizing rotated familiar objects. *Psychonomic bulletin & review*, 16, 5, Volume 16, Issue 5, 832–838.

PEACHY, D. 1986. Modeling waves and Surf. *In Proceedings of SIGGRAPH August 1986, ACM Press / ACM SIGGRAPH*, 65–74, 1986

PREETHAM, A.J., *Practical Analytic Model for Daylight*. University of Utah Category: Research <https://www.cs.utah.edu/~shirley/papers/sunsky/>

SHEMDIN, O.H. Sept. 1990. Measurement of Short Surface Waves with Stereophotography. *IEEE Conference Proceedings on Oceans '90. Engineering in the Ocean Environment*. 568–571

STRANSKY, D., WILCOX, L.M., and ALLISON, R. 2014. Effects of Long-Term Exposure on Sensitivity and Comfort with Stereoscopic Displays *ACM Transactions on Applied Perception*, Vol. 11, No. 1, Article 2.

TODD, J. T., EGAN, E.J., AND PHILLIPS, F. 2014. Is the perception of 3D shape from shading based on assumed reflectance and illumination? *Iperception*. 2014; 5(6): 497–514. Published online 2014 Sep 18.

TSIRLIN, I., ALLISON, R.S., WILCOX, L.M. May 2008. Stereoscopic transparency: Constraints on the perception of multiple surfaces. *Journal of Vision*, 8(5)

TURKEY, C., VIOLA ,I .,MICHELSEN, C ., SOLTESZOVA ,V. Dec. 2012 . A Perceptual-Statistics Shading Model .Issue No. 12 - vol. 18 ISSN: 1077-2626 pp: 2265-2274.

WAGEMANS, J., ELDER ,J ., KUBOVY,M.,PALMER,SE., PETERSON,MA., SINGH,M., VON DER HEYDT, R. 2012.A Century of Gestalt Psychology in Visual Perception: *I. Perceptual Grouping and Figure–Ground Organization*, Volume138(Issue6) 1172-1217

WANG, H., LIAO,M., ZHANG,Q., YANG,R AND TURK,G. 2009. Physically guided liquid surface modeling from videos. *ACM Trans. Graph.* 28, 3, Article 90 (July 2009), 11